

ELECTROCHEMICAL STUDIES OF THE CORROSION RESISTANCE OF BISMUTH TITANATE THIN FILMS DEPOSITED BY RF SPUTTERING

ESTUDIOS ELECTROQUÍMICOS DE LA RESISTENCIA A LA CORROSIÓN DE PELÍCULAS DELGADAS DE TITANATO DE BISMUTO DEPOSITADO MEDIANTE SPUTTERING RF

Manuel Jonathan Pinzón Cárdenas^{*,**}, Jhon Jairo Olaya Florez^{*,**}, José Edgar Alfonso Orjuela^{*,**}

ABSTRACT

Pinzón Cárdenas M. J., J. J. Olaya Florez, J. E. Alfonso Orjuela: Electrochemical studies of the corrosion resistance of Bismuth titanate thin films deposited by RF sputtering. *Rev. Acad. Colomb. Cienc.*, 37 (1): 79-84, 2013. ISSN 0370-3908.

Thin films of Bismuth titanate were grown on stainless steel (316L) and titanium alloy (Ti6Al4V) substrates, using the magnetron sputtering technique. The surface morphology of these films was observed with a scanning electron micrograph (SEM). The electrochemical studies used to evaluate the corrosion resistance of the substrate-coating set were the potentiodynamic polarization (Tafel) tests and electrochemical impedance spectroscopy (EIS), both done in a solution of NaCl (3%) as an electrolyte. The SEM showed that the morphology of the coatings grown on a titanium alloy Ti6Al4V substrate were in general homogeneous with a smooth surface but with un-melted material in some regions, while the morphology of the thin films grown on stainless steel 316L was mainly granular, with the presence of a few holes or craters. The potentiodynamic polarization curves showed that the corrosion resistance of the coated samples was better than that of the bare substrate, because the corrosion current obtained from the coated samples was lower by two orders of magnitude than that exhibited by the uncoated substrates, and in addition the corrosion potential of the coated samples was greater than that of the bare substrate. The EIS test showed the presence of a passive thin film of titanium oxide on the titanium alloy substrate.

Keywords: Bismuth Titanate, Thin films, Sputtering, Corrosion.

RESUMEN

Películas delgadas de Titanato de bismuto fueron crecidas sobre sustratos de acero inoxidable (316L) y aleación de titanio (Ti6Al4V), utilizando la técnica de magnetrón Sputtering. La morfología de estas películas fue

* Departamento de Ingeniería Mecánica y Mecatrónica – Universidad Nacional de Colombia, Bogotá, Colombia

** Departamento de Física – Universidad Nacional de Colombia, Bogotá, Colombia. E-mail: jealfonsoo@unal.edu.co

*** Grupo de Ciencia de Materiales y Superficies, Universidad Nacional de Colombia, Bogotá, Colombia

observada con microscopio electrónico de barrido (MEB). Los estudios electroquímicos utilizados para evaluar la resistencia a la corrosión del conjunto substrato-recubrimiento fueron la prueba de polarización potenciodinámica (Tafel) y la espectroscopía de impedancias electroquímicas (EIS), ambas pruebas fueron hechas en una solución de NaCl (3%) como electrolito. El MEB mostro que la morfología de los recubrimientos crecidos sobre substratos de aleación de titanio Ti6Al4V fue homogénea en general con una superficie suave pero con presencia de material sin fundir en algunas regiones, mientras que la morfología de las películas crecidas sobre acero inoxidable 316L fue principalmente granular, con la aparición de algunos cráteres. Las curvas de polarización potenciodinámica muestran que la resistencia a la corrosión de las muestras recubiertas fue mejor que la de las muestras sin recubrir ya que la corriente de corrosión obtenida de las muestras recubiertas fue dos órdenes de magnitud menor que la exhibida por las no recubiertas, adicionalmente el potencial de corrosión fue mayor en las recubiertas que en las no recubiertas. El ensayo de EIS mostro la presencia de una capa pasiva de óxido de titanio en la superficie de los substratos de aleación de titanio.

Palabras clave: Titanato de bismuto, películas delgadas, Sputtering, Corrosión.

1. Introduction

Bismuth titanate compounds (Bismuth titanate) are present in different crystalline configurations [1], such as sillenite [2], aurivillius (Layered-Perovskite) [3, 4], and pyrochlore [5], as well as in the amorphous phase [6]. These configurations have been studied extensively for many years due to their versatility in fields such as electronics and optics. For instance, the sillenite structure ($\text{Bi}_{12}\text{TiO}_{20}$) exhibits high photocatalytic activity in many reactions as a photo-degradation of methyl orange under UV-light [7], and also has photorefractive and photoconductive properties, which make it an optically active material and allow it to exhibit electro-optic, piezoelectric, and elasto-optic effects that are interesting for use in applications such as optical memories and dynamic holography [8, 9]. Meanwhile, the aurivillius phase of bismuth titanate ($\text{Bi}_4\text{Ti}_3\text{O}_{12}$) exhibits interesting properties at high temperatures (≤ 948 K), such as piezoelectricity and ferroelectricity, making it attractive for devices such as transducers and actuators, as well as for the automotive, aeronautic, and aerospace industries [3]. Furthermore, thanks to its reversible polarization, high dielectric constant, and electro-optic switching behavior, this compound is the object of special attention for applications such as non-volatile memories, capacitors of dynamic random-access memories, optical displays, and pyro-electric devices [10, 11]. The pyrochlore structure ($\text{Bi}_2\text{Ti}_2\text{O}_7$) has been the object of studies intended to take advantage of its optical properties and photocatalytic activities under visible-light [12]. Other research in this direction has proposed this compound as a material for use in the fabrication of advanced MOSFET transistors, taking advantage of its permittivity (relatively high) and low current leakage [13]. The foregoing information recounts a small part of the large number of studies done on the structural behavior, optical properties, and electrical properties of bismuth titanate. However, the number of studies devoted to the corrosion resistance and the electrochemical behavior of these materials is still very small. Therefore, in the present

paper we present the results of the corrosion resistance of bismuth oxide grown in the form of a thin film.

2. Experimental Details

The equipment used to grow Bismuth titanate thin films was an Alcatel HS 2000 RF sputtering system with a balanced magnetron 4" in diameter. The Bismuth titanate thin films were obtained from a 4" x 1/4" $\text{Bi}_4\text{Ti}_3\text{O}_{12}$ (99.9%) stoichiometric target. The parameters used during the deposition process were: base pressure 4.0×10^{-5} mbar, total working pressure 7.4×10^{-3} mbar, power applied at the target 150W, substrate temperature 623K, gas flow (Argon) 20 sccm, deposition time 30 min., and target-substrate distance 2". The preparation of the samples was carried out in the following order: cleaning of the samples by immersing them in isopropyl alcohol in an ultrasonic bath for 5 min., drying (with dry air), mounting of the samples on the galvanic cell, and finally placing the galvanic cell inside a Faraday cage in order to minimize the effects of the magnetic and electrical fields in the environment. Analysis of the potentiodynamic polarization curves was done with GamryEchem Analyst software. The equipment used to carry out the potentiodynamic polarization tests and the electrochemical impedance spectroscopy (EIS) was a Gamry Instruments reference 600 potentiostat with a three-electrode configuration. The reference electrode used in this test was a Saturated Calomel Electrode (SCE), accompanied by a Platinum electrode as an auxiliary electrode, and as working electrodes the samples were used. For both corrosion tests a 3% solution of NaCl was used.

3. Results and Discussion

Under the experimental conditions in which the bismuth titanate thin films ($T_s = 623$ K) were grown, the XRD studies did not show a crystalline structure, because the temperature needed for crystallization was not reached, neither in the aurivillius nor in the pyrochlore phase (> 773 K) [14, 15].

Furthermore, annealing was not carried out, due to the fact that the sensitization temperature of the stainless steel substrate and the exposition time of the sample to this temperature didn't allow it, and neither was it done for the titanium alloy substrates, in order to maintain the same experimental conditions for both substrates.

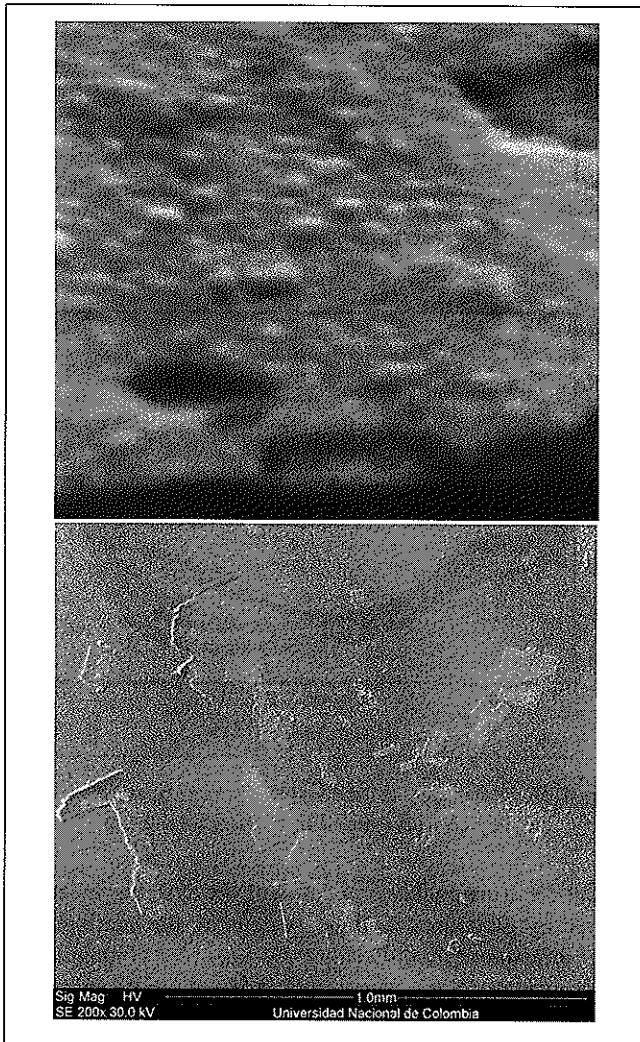


Figure 1. SEM of the surface of Bismuth titanate coating grown on stainless steel 316L (left) and titanium alloy Ti6Al4V (right).

The SEM (Fig. 1a) shows the surface of the Bismuth titanate coating on stainless steel 316L, in which one can observe that the morphology of the thin film is mostly granular; however, it also can be noted that there are a few holes or craters, which probably were formed through the re-sputtering effect. The grains that form the thin film have a size in the range of 0.028 to $0.17 \mu\text{m}^2$, while the holes or craters have a size in the range of 0.22 to $1.1 \mu\text{m}^2$. The SEM (Fig. 1b) shows the surface of the Bismuth titanate coating on titanium

alloy Ti6Al4V, in which one can observe that the morphology of the thin film is homogeneous. However, it can also be noted that there is some un-melted material, which probably is due to the fact that the temperature is not homogeneous on the surface of the substrate.

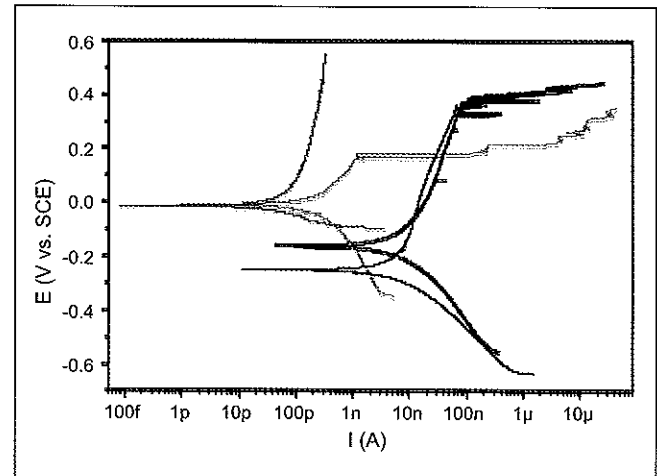


Figure 2. Potentiodynamic polarization curves obtained from stainless steel 316L substrate (black line), bismuth titanate thin film on stainless steel substrate (orange line), titanium alloy Ti6Al4V substrate (blue line) and bismuth titanate thin film on titanium alloy Ti6Al4V (green line).

The potentiodynamic polarization curves obtained from the samples of stainless steel 316L (Fig. 2, uncoated: black curve, and coated with BiTIO film: orange curve) show that the corrosion current (i_{corr}) decreases and the corrosion potential (E_{corr}) increases in the samples coated with bismuth oxide with respect to the uncoated samples. This is due to the fact that the thin film exhibits a protective behavior, since we found that the film surface is composed of Bi_2O_3 and TiO_2 , the latter oxide being a protection against corrosion [16, 17]. However, it is worth noting that although both i_{corr} and E_{corr} improved considerably with the application of the thin film onto the substrate surface, the appearance of possible pitting corrosion (current increase at the anodic region) occurs at a lower potential with the coating than without it. This behavior is due to the fact that the Bismuth titanate film is formed with holes through which the electrolyte penetrates.

Moreover, the potentiodynamic polarization curves obtained for the titanium alloy (Fig. 3, substrate: blue curve, and coated sample: green curve) shows that the coated sample exhibits a decrease in the corrosion current (i_{corr}) and an increase in the corrosion potential (E_{corr}) with respect to the uncovered samples, which is mainly due to the passive film

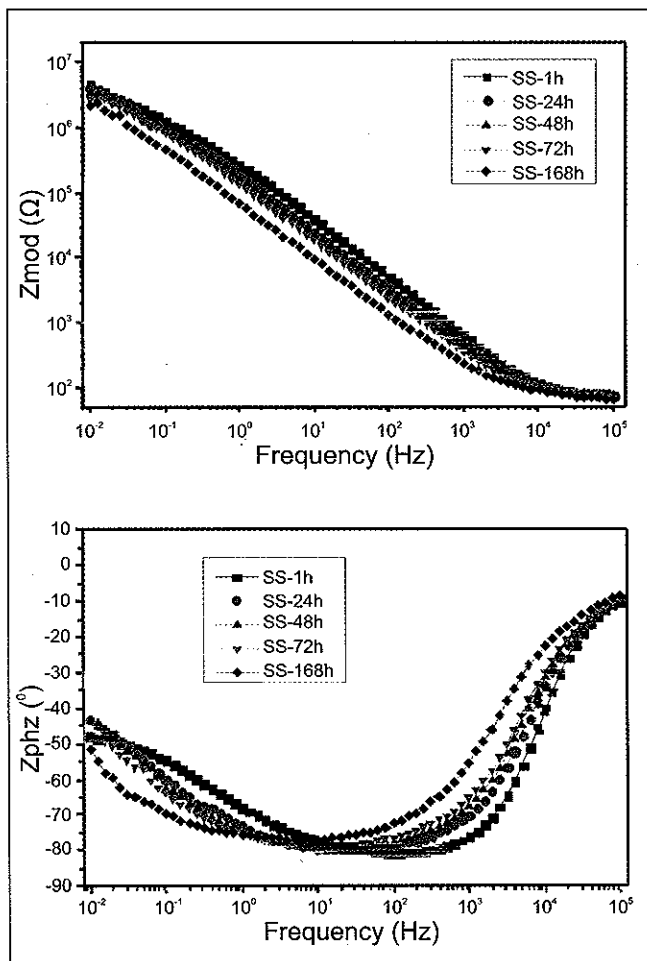


Figure 3. Bode diagram obtained from stainless steel 316L bare substratum.

of TiO_2 spontaneously grown on the titanium substrate, since it behaves as a protective thin film [18]. It is noteworthy that the behavior of the anodic region of the titanium alloy and of stainless steel is very different, since in the first substrate there is a passivation zone that is not present in the stainless steel substrate.

Bode plots for the stainless steel 316L substrate (Fig. 3) and the Bismuth titanate coatings (Fig. 4) show the immersion time in the corrosive electrolyte, which shows the presence of a relaxation time at high frequencies, representing the dielectric nature of the coating and the passive film formed on the substrate. This layer is generated by diffusing oxygen from the electrolyte onto the substrate surface through permeable paths (pores and defects), forming a thin film of low conductivity whose capacitance has a dielectric constant approximately to the coating. The variation in the height of the peak of the relaxation times at high frequencies suggests

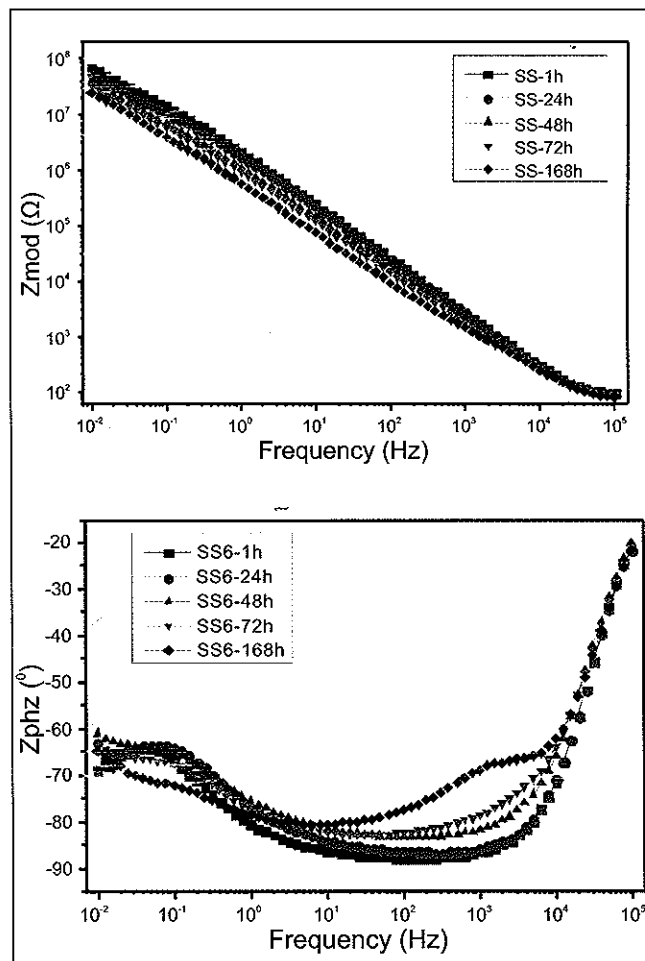


Figure 4. Bode diagram, obtained from stainless steel 316 substratum coated with a thin film of Bismuth titanate.

that the electrochemical properties of the systems tested are affected by the exposure time. In general, the coatings had higher impedance module values by one order of magnitude, at a frequency of 10^{-2} Hz, compared to the bare substrate. Such a Bode pattern possibly was due to the formation of a dense and compact structure that reduced the number of defects such as cracks, pinholes, and pores within the coatings, thereby further restricting corrosive electrolyte diffusion. The relatively small changes observed in the Bode spectra suggest considerable electrochemical stability for the coating due to the obstruction of defects by means of the corrosion products.

In summary, the steel substrate shows an increase in the impedance module when the immersion time is reduced, because the electrolyte diffusion through the coating took less time, producing a dense, passive, low-conductivity oxide film at the bottom of the permeable defects, exhibiting a ca-

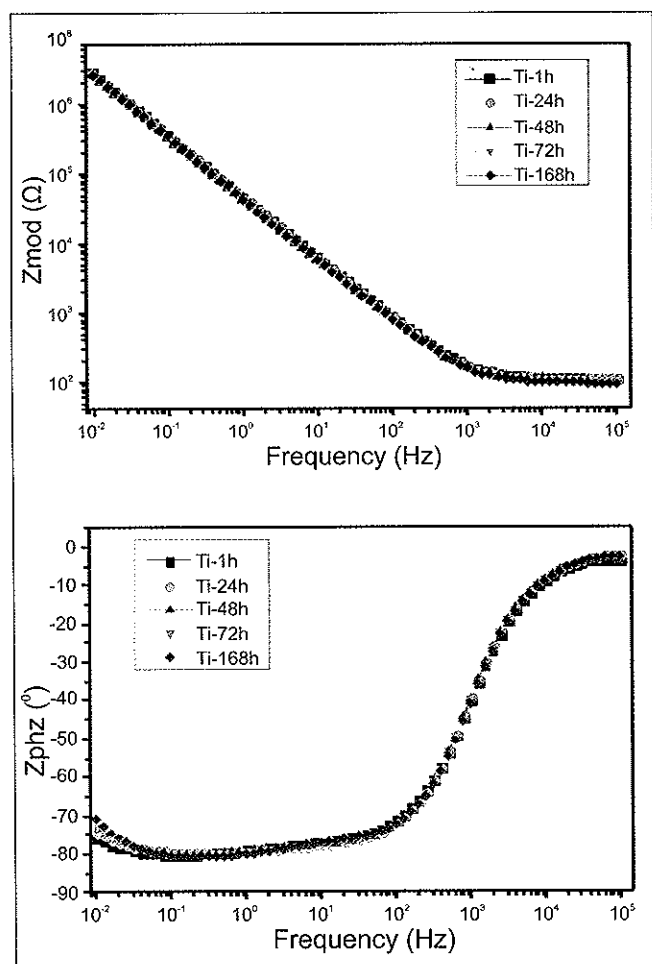


Figure 5. Bode diagram obtained for titanium alloy Ti6Al4V bare substratum.

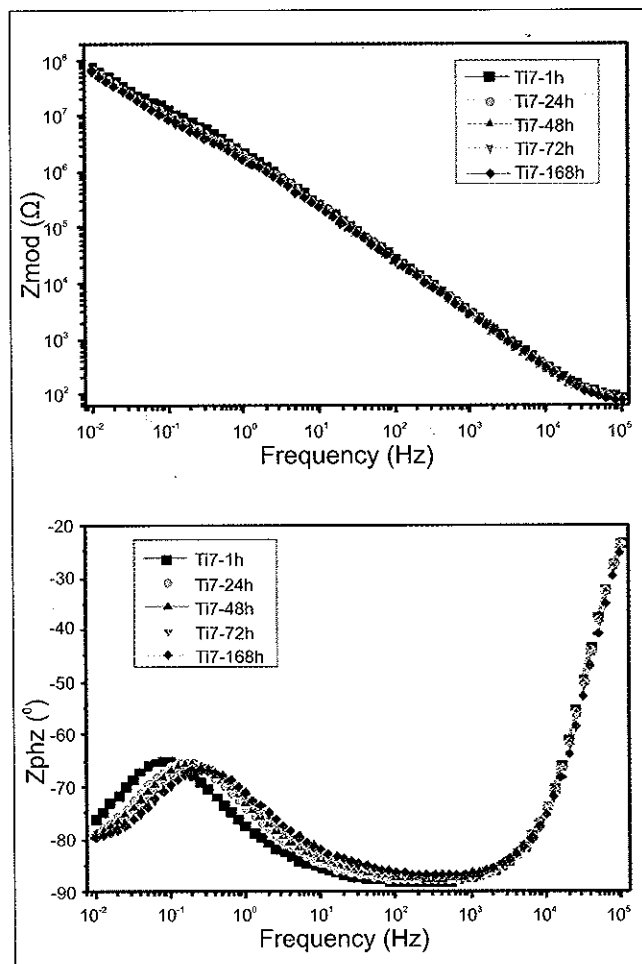


Figure 6. Bode diagram obtained for titanium alloy Ti6Al4V substratum coated with a thin film of Bismuth titanate..

capacitive behavior very similar to that of ceramic coatings. This behavior led to substrate surface passivity, which could dominate the corrosion process at the coating/substrate interface. However, increased immersion time expands the area of the pores in the coating, producing greater penetration of the corrosive solution toward the substrate surface, which produces localized corrosion.

A similar Bode pattern was seen for the titanium alloy Ti6Al4V substrate (Fig. 5) and the Bismuth titanate coatings (Fig. 6). However, the plots show one constant time, representing the capacitive response of the coating and the passive titanium alloy film. The relaxation time position remains unchanged, indicating no significant degradation of the coating as a function of testing time. The film deposited on Ti6Al4V exhibited the highest impedance module ($\sim 7 \times 10^8 \Omega$ at 10^{-2} Hz) of all the coatings evaluated in this investigation,

probably due to the strong influence of electrochemically inert passive films formed on Ti6Al4V.

4. Conclusions

Bismuth titanate thin films were grown on stainless steel (316L) and titanium alloy (Ti6Al4V) substrates through the rf magnetron sputtering technique, and their corrosion resistance was assessed via electrochemical techniques (potentiodynamic polarization and electrochemical impedance spectroscopy). These films exhibited a granular morphology with few craters for the stainless steel 316L, and un-melted material for the titanium alloy Ti6Al4V substrate. The electrochemical mechanisms that explain the increase of the corrosion resistance for the coated titanium alloy substrate obey the formation of the TiO_2 passivation layer, whereas for the coated stainless steel substrate the pitting current is due to

the penetration of the electrolyte through the holes present on the surface of the films.

Acknowledgments

The authors are grateful to the Universidad Nacional de Colombia for its financial support grants through project 15059 of the DIB, and for European Union FP7-NMP EU-Mexico program under *grant agreement* n°263878.

References

- [1] K. Sardar, R.I. Walton, (2012), Hydrothermal synthesis map of bismuth titanates, *J. Solid. State. Chem.*, **189**, 32 - 37.
- [2] V.M. Skorikov, Yu. F. Kargin, A.V. Egorysheva, V.V. Volkov, M. Gosponidov, (2005), Growth of Sillenite-structure single crystals, *Inorg. Mater+*, **41**, S24 - S46.
- [3] T. Jardiell, A.C. Caballero, M. Villegas, (2008), Aurivillius ceramics $\text{Bi}_4\text{Ti}_3\text{O}_{12}$ based piezoelectrics, *J. Ceram. Soc. Jpn.* **116**, 511 - 518.
- [4] W.F. Yao, X.H. Xu, H. Wang, J.T. Zhou, X.N. Yang, S.X. Shang, B.B. Huang, (2004), Photocatalytic property of perovskite bismuth titanate, *Appl. Catal. B-Environ.* **52**, 109 - 116.
- [5] I. Radosavljevic, J.S.O. Evans, A.W. Sleight, (1998), Synthesis and structure of pyrochlore-Type Bismuth titanate, *J. Solid. State. Chem.*, **136**, 63 - 66.
- [6] S. Kojima, A. Hushur, F. Jiang, S. Hamazaki, M. Takashige, M.S. Jang, S. Shimada, (2001), Crystallization of amorphous bismuth titanate, *J. Non-Cryst. Solids.*, **293-295**, 250 - 254.
- [7] J. Hou, Z. Wang, S. Jiao, H. Zhu, (2011), 3D $\text{Bi}_{12}\text{TiO}_{20}/\text{TiO}_2$ hierarchical heterostructure, Synthesis and enhanced visible-light photocatalytic activities, *J. Hazard. Mater.*, **192**, 1772 - 1779.
- [8] A.V. Egorysheva, (2009), Atomic structure of doped sillenites, *Inorg. Mater+*, **45**, 1175 - 1182.
- [9] N.C. Deliolanis, E.D. Vanidhis, N.A. Vainos, (2006), Dispersion of electrogyration in sillenite crystals, *Appl. Phys. B.*, **85**, 591 - 596.
- [10] F. Soares-Carvalho, P. Thomas, J.P. Mercurio, B. Frit, (1997), $\text{Bi}_4\text{Ti}_3\text{O}_{12}$ Thin Films from Mixed Bismuth-Titanium Alkoxides, *J. Sol-Gel Sci. Techn.*, **8**, 759 - 763.
- [11] A.M. Umabala, M. Suresh, A.V. Prasadaraao, (2000), Bismuth titanate from coprecipitated stoichiometric hydroxide precursors, *Mater. Lett.*, **44**, 175 - 180.
- [12] J. Hou, S. Jiao, H. Zhu, R.V. Kumar, (2011), Bismuth titanate pyrochlore microspheres, Directed synthesis ad their visible light photocatalytic activity, *J. Solid. State Chem.* **184**, 154 - 158.
- [13] J. Harjuoja, S. Väyrynen, M. Putkonen, L. Niinistö, E. Rauhala, (2006), Crystallization of bismuth titanate and bismuth silicate grown as thin films by atomic layer deposition, *J. Cryst. Growth.*, **286**, 376 - 383.
- [14] Z. Wang, D. Sun, J. Hu, D. Cui, X. Xu, D. Wang, Y. Zhang, M. Wang, H. Wang, H. Chen, C. Fang, X. Liu, K. Wei, J., (2002), The reactive ion etching of $\text{Bi}_2\text{Ti}_2\text{O}_7$ thin films on silicon substrates and its image in atomic force microscopy, *Cryst. Growth.*, **235**, 411 - 414.
- [15] M. Sedlar, M. Sayer, (1996), Structural and electrical properties of ferroelectric bismuth titanate thin films prepared by the sol gel method, *Ceram. Int.*, **22**, 241 - 247.
- [16] J.E. Alfonso, J.J. Olaya, M.J. Pinzón, J.F. Marco, (2013), Potentiodynamic Polarization Studies and Surface Chemical Composition of Bismuth Titanate ($\text{Bi}_x\text{Ti}_y\text{O}_z$) Films Produced through Radiofrequency Magnetron Sputtering, *Materials*, **6**, 4441 - 4449.
- [17] J. Pan, D. Thierry, C. Leygraf, (1996), Electrochemical impedance spectroscopy study of the passive oxide film on titanium for implant application, *Electrochim. Acta.*, **41**, 1143 - 1153.
- [18] J. Pouilleau, D. Devilliers, F.Garrido, S. Durand-Vidal, E.Mahé, (1997), Structure and composition of passive titanium oxide films, *Mat. Sci. Eng. B.*, **47**, 235 - 243.